Systems dynamic model of wear evolution for sheaves used in oil and gas hoisting operations

To cite this article: S Barua and I El-Thalji 2023 *IOP Conf. Ser.: Mater. Sci. Eng.* **1294** 012039

Systems dynamic model of wear evolution for sheaves used in oil and gas hoisting operations

S Barua* and I El-Thalji

Department of Mechanical and Structural Engineering and Material Science, University of Stavanger, Stavanger, Norway.

* Corresponding author: b.soumya@stud.uis.no

Abstract. The global offshore drilling contracted fleet consisted of 378 jack-ups, 68 semisubmersibles and 73 drillships, according to Westwood Global Energy Group, as of September 2023. In most regions of the world, rig activity has picked up from increased operator demand and pushed the marketed utilization for jack-ups from 76% to 85%, semis from 60% to 80% and drillships from 82% to 90%. The utilization of a drilling rig depends on various factors, mainly drilling demand, rig capability and specifications, and rig efficiency and reliability. Worn sheave grooves can pull down the efficiency of a drive by 8% accelerate the wearing of ropes reduce rope life, increase maintenance costs, and the need for more frequent rope replacements. Wear depth for sheaves is typically measured as the depth of wear in the groove of the sheave, which indicates the extent to which the sheave has worn down over time. Research on surface wear of wire rope caused by the contact between the wire rope and the sheave has rarely been carried out. Upgrading Archard's Wear model is needed to provide a better estimation of wear depth for sheaves. Moreover, the wear coefficient shall be determined. Therefore, the purpose of this paper is to model the wear evolution caused by the sliding contact between the wire rope and the sheave. To achieve this purpose, case sheaves were purposefully selected, studied and modelled using both the analytical and simulation modelling approaches.

1. Introduction

Oil and gas drilling operations involve complex machinery and equipment subjected to extreme conditions that can result in significant wear and tear. Sheaves, as type of pulleys, play a critical role in these operations by supporting and guiding cables or ropes used for lifting heavy loads, such as drill pipes and casings, as illustrated in Figure 1. In general, the travelling block is connected to the drawworks by a cable that ascends to the crown block at the top of the derrick from the drawworks (situated on or close to the main platform). The friction and mechanical stress experienced by sheaves from continuous rotation with loads during drilling operations lead to wear and eventual degradation of their performance. As a result, timely maintenance and replacement of sheaves are essential to ensure safe and efficient drilling operations.

The wire and the rope drive, often known as the sheave, are a wire rope drive's main part. However, the ropes are generally more prone to failure since they have a smaller cross-sectional area and are often subjected to fretting, fatigue, and abrasive wear [1]. Due to this, the wire rope has received the majority of attention in the tribological studies supporting wire rope drives [2,3] while the sheaves have often received far less significance.

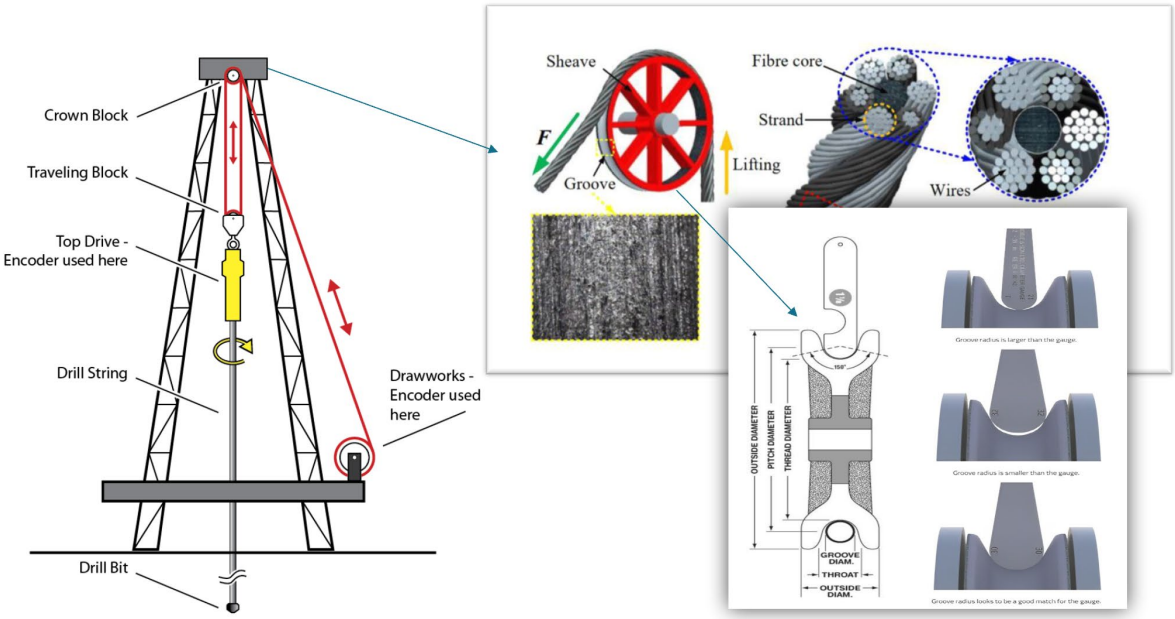

Figure 1. Sheave in drilling rig.

The sheave can also be worn out as abrasive wear act as failure mechanism in the sheave groove. The most common method to monitor the sheave health today is limited to visual inspections and manual groove measurements. The condition monitoring or predictive maintenance techniques are not applied yet. Thus, the purpose of this paper is to build a model that mimics the wear evolution caused by the sliding contact between the wire rope and the sheave. To achieve this purpose, case sheaves from the real-world were purposefully selected, studied and modelled using both the analytical and simulation modelling approaches. The developed model upgraded the Archard's Wear model [4] to provide a better estimation of wear depth for sheaves and estimated the wear coefficient for sheaves.

In the following section, the case studies and simulation models are presented. In section 3, the main results of the analytical and simulation models are presented and discussed, followed by some conclusions about the most sensitive parameters in sheave wear evolution process.

2. Materials and methods

In this section, the general wear theory and contributions toward rope and sheave wear are reviewed. Then, the analytical model to estimate the wear depth in sheaves are presented, together with the selected case study. Finally, the system dynamics model that combine the analytical model with actual operating conditions are presented.

2.1. Wear models for sheaves

In order to detect any signs of wear in the grooves that could lead to rope abrasion, pinching, or bird-caging, regular measurements of sheave groove are taken using two distinctive features – Groove depth and Groove radius. While groove depth of describes the vertical distance between the groove's deepest point and a reference plane (Figure 2), measuring groove radius ensures that sheave groove does not become too wide (overworn) or too narrow (aggregates rope pinching).

There are six distinct kinds of wear that can be characterized: abrasive; adhesive; fatigue; impact by erosion; corrosive; and electrical-arc-induced wear [5]. Corrosion and fretting are two additional typically highlighted wear modes. However, according to Hong et al., the industry's main wear mechanisms are abrasives, fatigue, and adhesives [6]. Metal-to-metal sliding contact during rope-sheave interaction is dominantly abrasive, while at the beginning the wear is adhesive. It is possible to model abrasive and adhesive wear using Archard's wear equation [4], while to model fatigue wear,

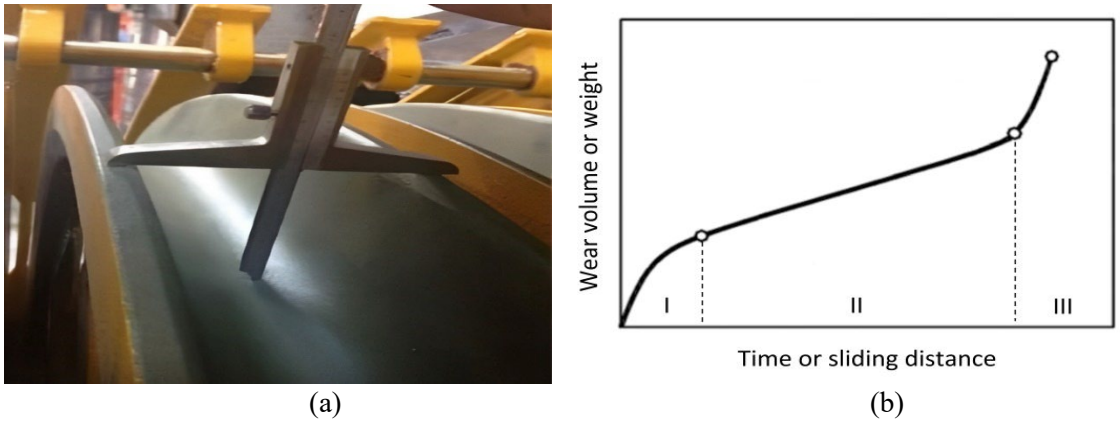

(a) (b)

Figure 2. a) Measurement of groove depth (Source: Case Company) and b) Typical Wear curve with I. Transient II. Steady-state and III. Wear-out stage of wear phenomenon [4]

Coffin-Manson-type relation of fatigue fracture is more suitable [7]. Archard's wear equation calculates the volume of wear per unit sliding distance (q) depending on Normal Load (F), and the hardness of the softer surface (H), then Archard's wear equation is given as –

$$q = \frac{K \times F}{H} \quad (1)$$

where, K is a dimensionless constant. The wear coefficient (k) can be calculated by dividing the K over H (k = K/H).

In terms of wear depth (h), the Archard's equation can be utilised by considering the sliding distance (s) and contact pressure per unit area (p), then the wear depth equation is given as following:

$$h = k \times p \times s \quad (2)$$

Archard's seminal work in 1953 laid the foundation for understanding wear in sheave and rope interactions. He posited that wear is proportional to applied load and inversely proportional to the hardness of the softer surface. This equation has been widely used in engineering practice to estimate wear rates [8]. He also introduced the concept of a running-in stage, during which wear rates tend to decrease to a constant value after initial higher wear [9].

Building upon Archard's model, Varenberg's recent work extended the understanding of wear by considering the running-in stage. Varenberg incorporated surface topology data retrieved from the bearing ratio curve, also known as the Abbott-Firestone curve, into a modified Archard's equation. This modification allows for more accurate wear measurements during the running-in period and steady-state wear [4].

Hutchings and Shipway [5] emphasized that wear in sheave and rope systems is governed by various factors, including mechanical stresses, thermal and chemical properties, and surface interactions. Their research highlights the complex interplay between these factors and how they evolve over time as the contact progresses. According to them, there is more than one wear mechanism at work when metals slide against each other, and as the sliding conditions change, the relative value of each mechanism changes.

Oksanen et al. conducted extensive wear mechanism analyses in sheave grooves. Their work revealed deformation tongues from plastic deformation, crack propagation, and contact pressure-induced wear. They noted that initial contact with wire rope occurs at groove flanges, leading to diagonal cracks and deep pits in the material [10,11].

Hamblin and Stachowiak contributed to understanding environmental effects on wear, finding that dry conditions lead to adhesive wear and corrosion, while wet conditions accelerate corrosion wear and surface pitting [12].

Kato [7] underscored the multiparameter-sensitive nature of wear. Wear is influenced by numerous contact factors, including material properties, stress, contact angle, sliding speed, suspension stiffness, lubrication, and environmental conditions. Kato's research highlighted that metal-to-metal wear is dominantly adhesive at the beginning, and then the wear mode changes to abrasive wear as the microstructure and micro geometry change forms a rubbing texture on the contact surface.

Kulinaowski et al. addressed the significance of the friction coefficient in sheave and rope wear, particularly in realistic industrial conditions. Their research focused on measuring the operational friction coefficient of belt/drum drives under varying speeds and loads, highlighting the impact of friction on wear [13]. Hrabovský et al. developed a methodology to determine the friction coefficient in sheave grooves, noting variations based on load, lubrication, and groove type [14].

Shi et al. used finite element analysis to explore the relationship between wrap angle, pretension, contact force, and wear [15]. Guo et al. introduced the concept of the "global dynamic wrap angle," providing insights into how rope behaviour changes as it approaches and unwinds from the wrap angle [16]. Olszyna et al. examined the impact of wear on the geometrical parameters of sheave grooves, emphasizing the role of pulley positioning and rope design in influencing wear patterns [17].

Nabijou and Hobbs studied the effect of rope core type on friction, finding that it did not significantly affect the effective friction coefficient [18]. Studies by Goto and Amamoto as well as Xiangdong et al. explored wear behavior under varying loads and dynamic conditions. Goto and Amamoto's experiments revealed the transition from mild to severe wear and "quasi-mild wear"[19]. Xiangdong et al. observed the inverse relationship between friction coefficient and sliding distance and the evolution of wear debris [20].

Liu et al. introduced an automated machine vision-based system for wear detection in sheave grooves, providing a non-contact and precise method for assessing wear in industrial settings [21]. Ge and Zhang et al. investigated the frictional behavior of ropes under different conditions, considering parameters such as velocity, pressure, and tension force [22, 23]. Their research contributed to a better understanding of the complex relationship between these factors and friction.

In summary, the literature reviewed here underscores the multidimensional nature of wear in sheave and rope systems, emphasizing the importance of factors like load, friction, surface topology, and environmental conditions. These factors are accounted for in the dimensionless wear coefficient, k, in Archard's wear equation. Hence, the value of k will be different from case to case.

2.2. Analytical Model

In order to formulate the mathematical model that estimates the wear depth per revolution, the contact pressure against sheave groove (Figure 3), sliding distance and wear coefficient are required, which can be formulated as-

$$\frac{\text{Wear depth}}{\text{Circumference of sheave groove tread}} = \frac{\text{Wear coefficient}}{\text{Hardness of sheave groove}} \times \text{Peak pressure against groove} \times \text{Relative sliding length per revolution}$$

2.2.1 Properties of wire rope and hoisting system. Circumference of sheave groove, contact pressure and total sliding distance depend on the contact's geometrical and material properties. In Table 1, the rope diameter, grade, cross-section, breaking load, tension, and number of falls are listed. Moreover, the sheave properties are listed such as hoisting capacity, sheave efficiency, sheave bending pitch diameter, and sheave hardness.

We have considered (1) Properties of wire rope against which the sheaves are in a relative sliding motion, (2) the properties of the hoisting system itself, and (3) the load and sliding distance experienced by the sheaves (Load-level data).

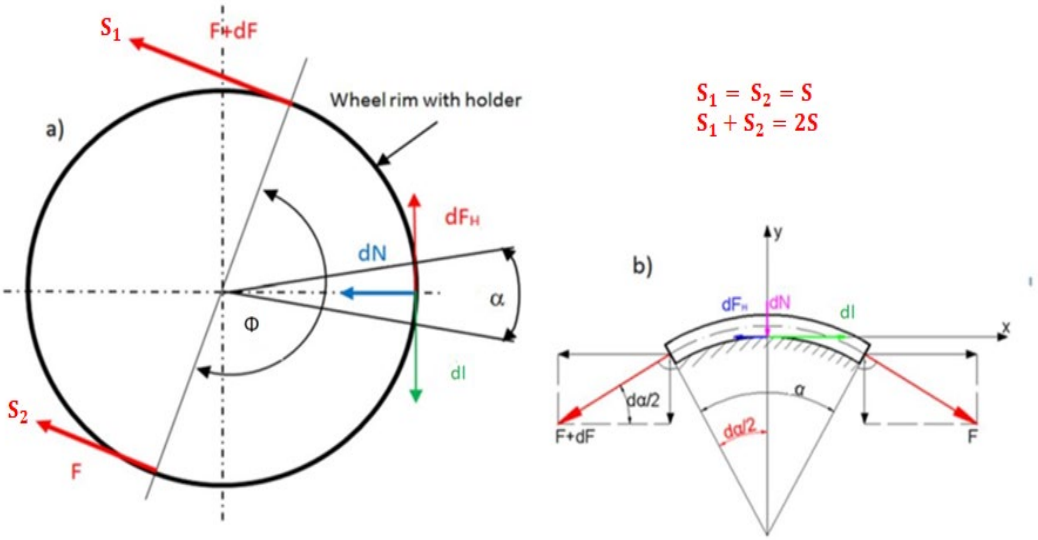

Figure 3. (Left) Schematic diagram of rope mechanics bent over sheave, (Right) Mechanics of rope power transmission on the elementary section of the sheave [24]

Table 1. Rope and Sheaves' properties.

Properties	Symbol	Value with unit
Nominal Rope Diameter	d	50.8 mm
Rope Grade (specific material grade or quality of a wire rope)	R_m	1960 MPa
Minimum Breaking Load (load endured by a rope without breaking)	F_u	1760 kN
Metallic Cross-Section (collective cross-sectional area of the metallic elements/wires)	A	1159 mm^2
Nominal Cross-Section (rope's overall cross-sectional area)	A_n	2027 mm^2
Nominal Rope Tension (pulling force applied to the wire rope)	S	72.1 kN
Rope falls (number of wire rope segments supporting the load)	n_f	16
System hoisting capacity	F_{max}	11122 kN/1250 short tons
Sheave bending pitch diameter (where the rope wraps around the sheave)	D_s	1735 mm
Hardness of sheave groove (toughness of sheave interior to resist wear and deformation)	H	2453 MPa/250 HB
Sheave efficiency (a measure of effectiveness to transmit power to wire rope)	η_s	98%
Kinetic friction coefficient	μ_k	0.1
Peak pressure coefficient	ψ_p	5
Coefficient of Nonlinear Elastic Modulus	C	434618649 MPa
Exponent of the Non-linear Elastic Modulus	β	3
Tangential Elastic Modulus (at 20% load)	$E_t^{20\%}$	102675 MPa

The circumference of sheave groove tread (O) which is the entire area of the sheave groove tread that comes into contact with the rope (in mm^2), can be calculated by,

$$O = \pi \times (D_s - d) \quad (3)$$

2.2.2 Load and contact pressure: To estimate the Peak pressure against Groove (p), which is the highest level of pressure encountered by the wire rope when it comes into contact with the groove of the sheave, the following four properties are needed: Peak pressure coefficient (ψ_p), Nominal rope tension (S),

Sheave bending pitch diameter (D_s), and Nominal Rope Diameter (d). Thus, the Peak pressure against Groove (p) is given as:

$$p = \frac{\psi_p \times 2 \times S}{(D_s - d) \times d} \quad (4)$$

The Peak pressure coefficient (ψ_p) is the ratio of peak pressure to nominal pressure experienced by the system. As specified in [26], we will use the peak pressure coefficient value of 5 in this model. However, total rope tension is the product of the Nominal rope tension (S) acting on each side of the sheave (Figure 2), which can be deduced the following equation:

$$S = \frac{F}{n_f} \quad (5)$$

Here actual hook load F refers to the total of actual load carried and the weight of the attachments (such a trolley or lifting tackle) linked to it and is calculated as -

$$F = \varphi \times \text{System hoisting capacity } (F_{max}) \quad (6)$$

Here, Φ is the load percentage rating of the hoisting system and in our case, it is 10.4%.

2.2.3 Total Sliding Distance: The second variable in the wear depth equation is the relative sliding length per revolution (δ_O), which is the distance the wire rope travels relative to the sheave or pulley during a full rotation and can be calculated as:

$$\delta_O = \frac{\text{Nominal rope tension (S)} \times \text{Sliding distance at groove tread (s)}}{\text{Nominal Cross-Section } (A_n) \times \text{Actual tangential E-modulus } (E_t)} \quad (7)$$

The nominal rope tension (S) is already previously calculated and the nominal cross section area, which is the overall cross-sectional area (mm^2), including metallic and non-metallic components, can be easily calculated by:

$$A_n = \frac{\pi d^2}{4} \quad (8)$$

However, to estimate the sliding distance at groove thread (s), which is the linear distance the rope travels along the groove tread during each cycle (in mm), the sliding arc angle (α) is required, which is an angular distance covered by the rope as it slides along the sheave's groove tread (in radians). the sliding arc angle (α) by itself depends on the Sheave efficiency (η_s) and Kinetic friction coefficient (μ_k). Sheave efficiency (η_s) measures power transmission effectiveness taking into account friction and deformation losses. As per industry norm, we will consider 98% efficiency for the sheaves in our model. Kinetic friction coefficient (μ_k) represents friction between the sheave and wire rope. As specified by Timoshenko, the metal-to-metal friction is kinetic, and deduced that the value of this kinetic friction coefficient is 0.1 [27]. Therefore, the Sliding arc angle (α) can be estimated by:

$$A\ (\text{rad}) = \frac{1}{\mu_k} \times \ln\left(\frac{1}{\eta_s}\right) \quad (9)$$

Thus, the sliding distance at groove tread (s):

$$s = \alpha \times \frac{D_s - d}{2} \quad (10)$$

To estimate the relative sliding length per revolution (δ_O) still the actual tangential E-modulus (E_t) is required. The actual tangential E-modulus measures wire rope's modulus of elasticity in the tangential direction, using the following equation:

$$E_t = \beta \times \sigma \times \left(\frac{C}{\sigma}\right)^{\frac{1}{\beta}} \quad (11)$$

Tangential Elastic Modulus (E_t) is a quantitative indicator of a material's stiffness within the plastic deformation range, calculated based on the gradient of the stress-strain curve. Its value can vary depending on the specific measurement location. Exponent of the Non-linear Elastic Modulus (β) is a parameter that shapes the curve representing the relationship between stress and strain in the wire rope. Due to geometrical considerations of wire ropes, value of 3 has been selected as the exponent of non-

linear elastic module [25]. In some cases, the modulus of elasticity may not remain constant but may vary with the applied load. The Coefficient of Nonlinear Elastic Modulus (C) accounts for the wire rope's nonlinearity in the relationship between stress and strain.

In general, the actual load carried by the hoisting system is 20% of its' maximum capacity and thus the Coefficient of Nonlinear Elastic Modulus is derived from:

$$C = \sigma_{20\%} \times \left(\frac{E_t^{20\%}}{\beta \cdot \sigma_{20\%}}\right)^{\beta} \quad (12)$$

Rope stress, σ is the ratio of the Internal force (Nominal Rope Tension, S) and the total metallic cross-sectional area (A).

2.2.4 Wear coefficient and wear depth: Assuming a set value of wear coefficient k_w and recalling the values of peak pressure against groove and relative sliding distance per revolution from Equations 4 and 7 respectively, the amount of relative radial wear in the groove for a single revolution can be retrieved using the Archard's wear equation as-

$$h/O = \frac{k_w}{H} \times p \times \delta_O \text{ (mm/rev.)} \quad (13)$$

Ton-km and $\text{Ton}^2 - \text{km}$ are two important parameters that are logged by rig systems for fatigue calculations, and we can apply these parameters in deriving the average load and sliding distance. Ton-km represents the movement of one metric ton of cargo over a distance of one kilometer, while $\text{Ton}^2 - \text{km}$ measures the square of the weight of goods (in metric tons) multiplied by the distance travelled.

$$\frac{Ton^2-\text{km}}{\text{Ton}-\text{km}} = \text{Average Load in Metric Tons} \quad (14)$$

$$\text{Total Sliding Distance} = \frac{\text{Ton}-\text{km}}{\text{Average Load}}$$

Thereby, the accumulated travelling length,

$$Z_{tot} = \frac{\text{Ton}-\text{km}}{\text{Average Load}} \quad (15)$$

Recalling the circumference of the sheave tread from Equation (3), we get the total number of sheave revolutions as -

$$n = i \times \frac{Z_{tot}}{O} \quad (16)$$

where, *i* is the Peripheral speed of a sheave, referring to the average velocity difference between the two falls as they rotate over a specific sheave which increases linearly as alternating increments occur between the traveling and the crown block. The peripheral speed of the rope determines the friction and wear of a particular sheave experience.

Table 2. Sheave number vs. peripheral speed chart

Crown block sheaves:	CB1	CB2	CB3	CB4	CB5	CB6	CB7	CB8
Peripheral speed (i):	2	4	6	8	10	12	14	16
Traveling block sheaves	TB1	TB2	TB3	TB4	TB5	TB6	TB7	TB8
Peripheral speed (i):	1	3	5	7	9	11	13	15

Finally, total wear depth in the groove can be determined from the value of wear per revolution by the sheave h/O multiplied by the total number of sheave revolution *n*, as shown in Equation (17) as –

$$h = n \times h/O \quad (17)$$

2.3. Case studies and Parameter Extraction

Based on the analytical model for wear evolution in sheaves, there are several sensitive parameters that shall be extracted in a practical manner, particularly, sliding distance and the wear coefficient.

The drilling operations may take several years to start and may go through breaks due to various reasons such as maintenance intervals, hot/warm/cold stacked conditions, etc. The key challenge in systematically estimating wear of a running system is to accurately derive the total number of revolutions while taking into account all the breaks and pauses. Original Equipment Supplier (OEM) supplied the values ton-km and ton^2-km from fatigue calculations which is vital to apply the devised mathematical model for finding accumulated wear.

The wear coefficient value of a specific case can be retrieved through several ways: (1) Analysis of design parameters and historical measurements, (2) Laboratory tests with similar loading conditions and wear environment and/, or (3) Finite Element Analysis or other numerical analysis tools, and (4) Experiential extraction by collecting the wear depth and the sliding distance. The last way was possible in this case study since there were two sets of data (As-born and one measurement logged after 8 years) available, with no measurements at the early stage of the wear duration. This resulted in the wear curve following a linear trend while the transient or running-in state not being represented in the wear curve.

As the change in the wear depth is measured over specific period and given the ton-km data, the specific wear coefficient could be extracted by taking the average of the individual sheave wear coefficients.

2.4. System dynamics simulation model

Estimating the wear evolution means that the wear depth will be calculated over time. Thus, a dynamic model that estimate wear depth every time unit (e.g, every hour) based on the analytical model is needed.

System dynamics modelling perfectly provide the change of specific variable over time in a time plot. It is almost same as putting the analytical model in a loop that calculate the wear depth value at each time unit over a specific time period. It is important to mention that when wear depth increases over time, the wear rate increases and that exponentially increase the future wear depth. This reinforcing phenomenon can be considered in system dynamics models, as shown in Figure 4.

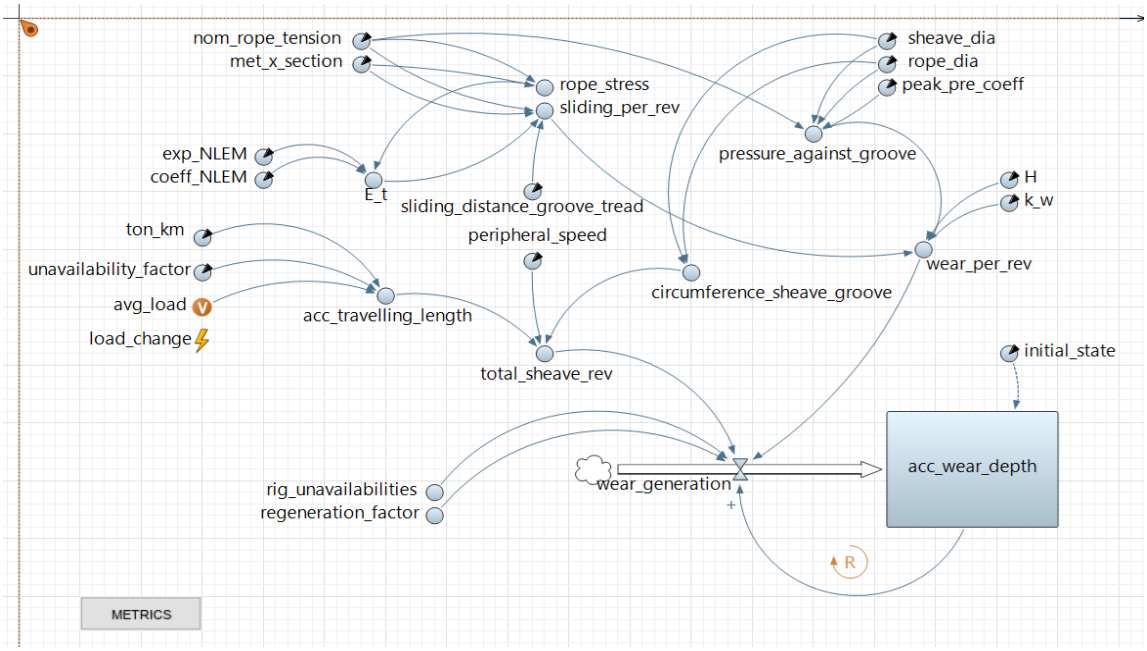

Figure 4. System dynamics simulation model for sheave wear depth.

AnyLogic simulation software was used to incorporate the mathematical model into a system dynamic simulation model of wear phenomena. The parameters and equations used in the analytical model are simply placed in the dynamic model through parameters and dynamic variables respectively, while variable 'avg_load' was used to determine the average load from fatigue calculations and the event 'load_change' fluctuates the average load over a normal distribution. The simulation model was detrimental in terms of simplifying lengthy calculations, producing wear curve and dynamically view wear progression, testing the effect of variable parameters such as wear regeneration factor, load and sliding distance, and finally predicting the amount of wear.

Since numerical and design intensive simulation software are time-consuming and require a wide range of data as well as prior training, it was decided that AnyLogic would be a better option to proceed, since its fits the purpose and a model could be developed without requiring any additional data. At first, the current model was developed by introducing parameters 'rig_unavailabilities' and 'unavailability factor' in order to include the non-operational periods during the timeline. The simulation model made is simpler to derive the wear values in an accurate manner. Additionally, it was easier to change and add different parameters such as load, regeneration factor, etc. However, predicted wear in the future would are based on the condition that the operation will run continuously, without any stoppage or shutdowns.

3. Results and discussion

In this section, three results' categories are presented. First, the individual and average wear coefficients are extracted and presented. Second, the wear depth time plot is presented considering the operational and non-operational periods over 10 years. Third, the effect of the load variation is presented and discussed. The calculated values display the highest amount of wear for the Fastline sheaves whereas deadline sheaves experience no wear. This pattern pertains to the mechanics of wear in multi-sheave rope drives. As power is transferred from the input sheave to the output sheave, the peripheral speed increases to compensate for the drop in diameter and keep the wire rope at a constant linear velocity throughout the drive system, resulting in no rotation in Deadline sheaves while Fastline sheaves rotates at highest speed. The inconsistent distribution of logged wear along the sheaves, as well as occurrence of wear in the Fastline sheaves suggest that the positions of the sheaves were interchanged at some stage of the wear period during periodic maintenance programs.

The wear curve derived from analytical model resembles an almost linear trend (Figure 5). This behavior is expected since the transient state of wear was accounted for due to lack of measurement points. However, since Archard's wear equation is valid for long wear periods, the wear curve determined from the calculations can be viewed as realistic, even if it only displays the steady-state wear progression.

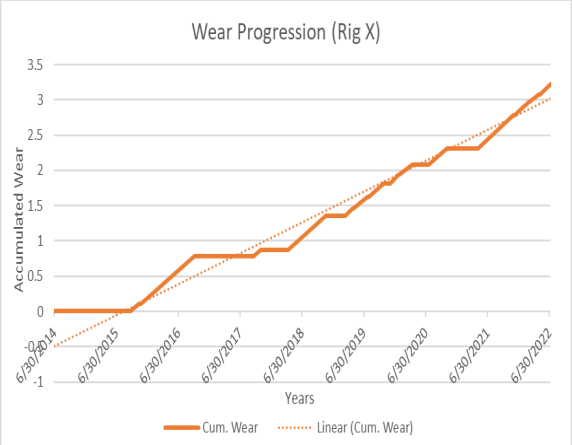

Figure 5. Projected Wear Curve for Sheave 5 in Rig X.

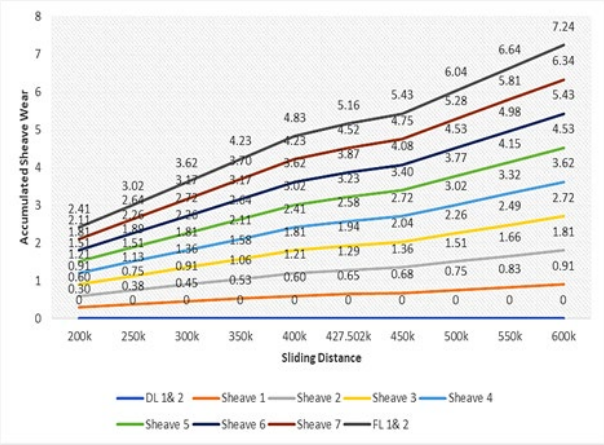

Figure 6. Average Load vs. Sheave Wear

It is visible from the Archard's wear model that wear depth is directly proportional to the load applied and total sliding distance. However, according to Hutchings and Shipway [5], while direct proportionality between sliding distance and wear is true (Figure 6), sheave wear is generally proportional to load applied for up to a point (Figure 7), usually until preliminary surface layers are worn off.

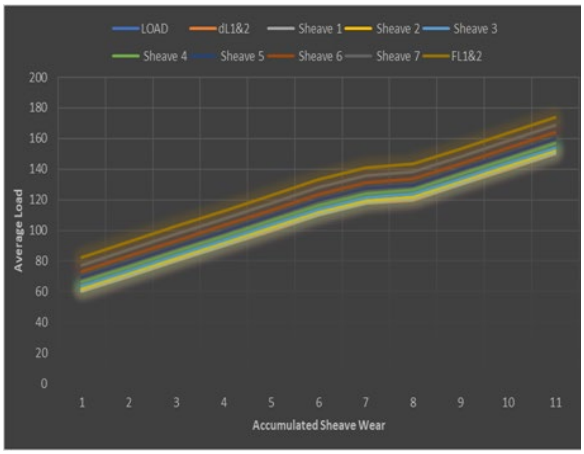

Figure 7. Sliding Distance vs. Sheave Wear

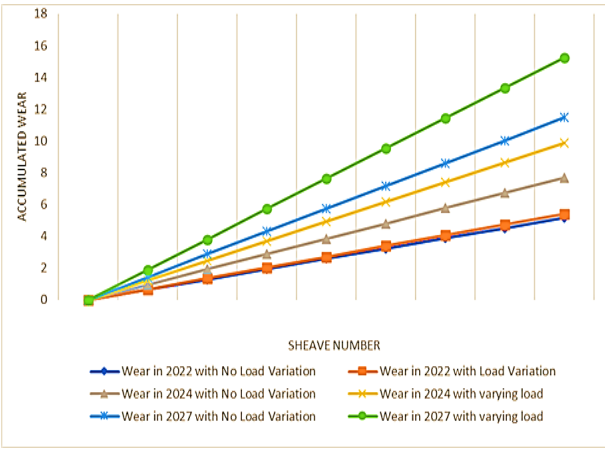

Figure 8. Predicted trend of Sheave Wear

The AnyLogic simulation software was useful to predict the amount of wear to be accumulated in any given number of years in the future (Figure 8). The data from the fatigue calculations provided the value of the average load carried by the crown block (Figure 9). However, using Anylogic it was possible to display the effect of load fluctuating over a given range (Figure 10), which is logical in terms of real-life operational scenario. Lastly, higher amount of wear resulted from fluctuating loads shed more light on the importance to consider real-life loading conditions and AnyLogic's capabilities to simulate them (Figure 11).

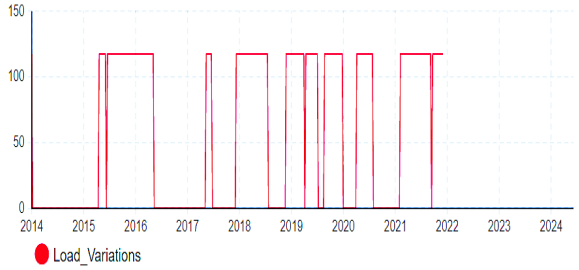

Figure 9. Average load throughout wear period

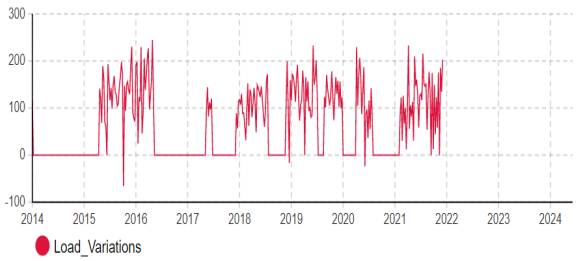

Figure 10. Fluctuating average load

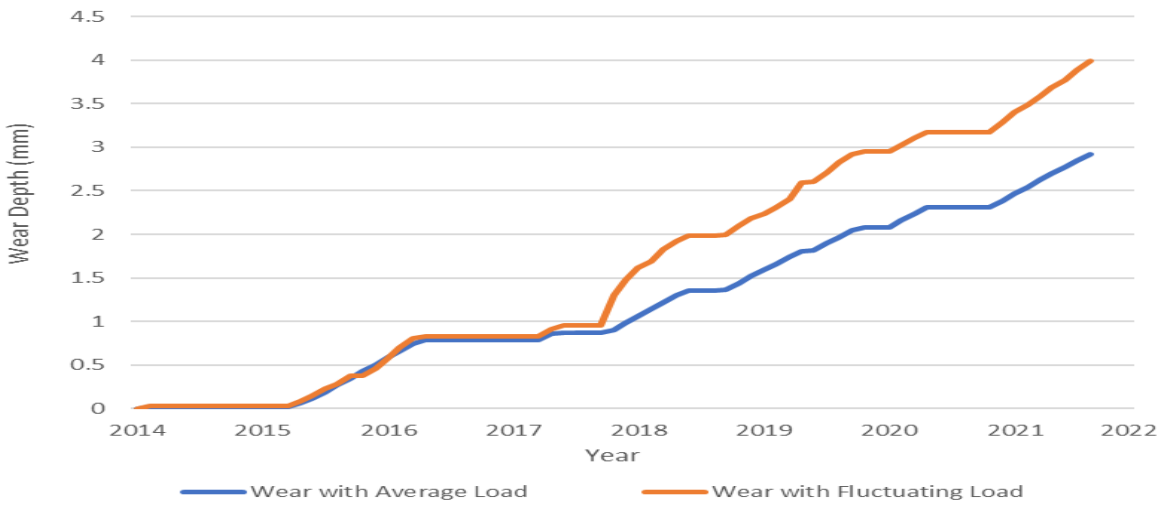

Figure 11. Wear with Average and Fluctuating Load

4. Recommendations for future work

Future studies should focus on improving data collection processes, particularly by incorporating multiple measurements over time on fixed reference points along the sheave's circumference. Techniques like non-contact laser profilometry and atomic force microscopy can be employed to measure wear based on surface roughness [5,28]. Most importantly, to address the limitations of the current methodology, future research should explore numerical modelling using tools like Ansys or Abacus [11]. This approach can provide a more comprehensive understanding of rope-sheave interactions and may lead to a more accurate estimation of sheave wear by considering both groove depth and groove radius changes.

5. Conclusion

The analytical model presented in this paper upgrades the general wear model to be more customised for sheave wear considering the sheave mechanics, geometrics, and properties. Then, the study was able to combine the real-world measurements with the analytical model to estimate the wear coefficient in a practical manner. It can be concluded that the wear coefficient is the most sensitive factor that should be carefully estimated and extracted. The system dynamic model enabled us to get the time plot of the wear depth and also model the third stage of the wear curve, known as the wear-out stage, which depends on the reinforcing phenomenon of the wear rate.

The research brings attention to several critical considerations and limitations in the development of the wear model and the overall study. Firstly, the model assumes uniform abrasive particle geometry and consistent material removal behavior, which may not align with real-world scenarios where irregular particle shapes and variable material removal are common. Additionally, the intricate nature of rope-sheave interactions presents a challenge, leading to the exclusion of groove radius measurements in favour, which has the potential to increase the accuracy of the projected wear. The study also makes an assumption regarding the maintenance strategy for sheave orientation (sheave orientations were changed but were not logged in records) due to limited operator verification. Furthermore, the research does not account for the influence of accumulated wear on wear rates, as quantifying the effects of wear debris remains a challenge. Lastly, the absence of measurements at the start of the wear period means that the model cannot represent the transient wear state, resulting in a linear wear curve trend. These limitations highlight opportunities for future research to delve deeper into these complexities and improve the accuracy of wear predictions in sheave systems.

References

[1] Feyrer K 2007 Wire Ropes: Tension, Endurance, Reliability, Springer
[2] Ridge I M L, Chaplin C R and Zheng J 2001 Effect of degradation and impaired on wire rope bending over sheave fatigue endurance. *Eng. Fail. Anal.* **8**(2), 173–87.
[3] Cruzado A, Hartelt M, Wäsche R, Urchegui M A and Gómez X 2010 Fretting wear of thin steel wires Part 1: Influence of contact pressure. *Wear* **268**(11–12), 1409–16.
[4] Varenberg M 2022 Adjusting for running-in: Extension of the archard wear equation. *Tribol. Lett.* **70**(2). https://doi.org/10.1007/s11249-022-01602-6
[5] Hutchings I and Shipway P 2017 Tribology: Friction and Wear of Engineering Materials. Butterworth-Heinemann, 2nd Ed., Elsevier.
[6] Hong W, Cai W, Wang S and Tomovic M 2018 Mechanical wear debris feature, detection, and diagnosis: A review. Chinese J. Aeronaut. **31**(5), 867–82.
[7] Kato K. *Classification of Wear Mechanisms/Models*. John Wiley & Sons, Ltd eBooks [internet]. 2014. p. 9-20. Available at: https://onlinelibrary.wiley.com/doi/abs/10.1002/9780470017029.ch2
[8] Archard J F and Hirst W 1956 The wear of metals under unlubricated conditions Proceedings of the Royal Society of London 2 236 (1206)397–410
[9] Archard J F 1953 Contact and Rubbing of Flat Surfaces, *J. Appl. Phys.* **124**(8)
[10] Oksanen V, Andersson P, Valtonen K, Holmberg K and Kuokkala V 2013 Characterization of the wear of nodular cast iron rollers in contact with wire ropes, *Wear,* **308**(1–2) 199-205
[11] Oksanen V Valtonen K Andersson P Vaajoki A Laukkanen A and Holmberg K 2015 Comparison of laboratory rolling–sliding wear tests with in-service wear of nodular cast iron rollers against wire ropes*. Wear,* **340–341** 73–81
[12] Hamblin MG and Stachowiak G 1995 Environmental and sheave material effects on the wear of roping wire and sheave. *Tribol. Int.* **28**(5), 307–15.
[13] Kulinowski P Kasza P and Zarzycki J 2021 *Identification of the operating parameters of the friction drum drive in industrial conditions* Eksploatacja I Niezawodność 31 23(1) 94–102
[14] Hrabovský L Fries J Kudrna L and Gaszek J 2022 Determination of the coefficient of friction in a pulley groove by the indirect method. *Coatings* **12**(5) 606.
[15] Shi X Pan Y Ma X 2017 Modeling and analysis of the rope–sheave interaction at traction interface, *J. Appl. Mech.* **84**(3)
[16] Guo Y Zhang D Feng C and Liu Y 2016 Dynamic creeping behaviors between hoisting rope and friction lining in friction transmission*, J. Vibroeng.* **18**(8)5010–28
[17] Olszyna G Sioma A Tytko A 2014 Laser Measurement System for the Diagnostics of Mine Hoist Components/Laserowy System Pomiarowy Do Diagnostyki Elementów Górniczych Wyciągów Szybowych, Arch. Mining Sci. **59**(2) 337–46
[18] Nabijou S Hobbs R E 1995 Frictional performance of wire and fibre ropes bent over sheaves, *J. Strain Anal. Eng. Des.* **30**(1) 45–57
[19] Goto H and Amamoto Y 2003 Effect of varying load on wear resistance of carbon steel under unlubricated conditions, *Wear* **254**(12) 1256–66
[20] Xiangdong C Peng Y Zhu Z Lu H Tang W and Zhang X 2022 Sliding Friction and Wear Characteristics of Wire Rope Contact with Sheave under Long-Distance Transmission Conditions *Mater.* **15**(20) 7092
[21] Liu S Ma D and Liu G 2022 Wear Detection System for Elevator Traction Sheave, J. Shanghai *Polar* Jiaotong University (Sci.) **27**(5) 706–14
[22] Ge S 1992 The friction coefficients between the steel rope and polymer lining in frictional hoisting. *Wear* **152**(1) 21–9
[23] Zhang Q Peng Y Zhu Z Tang W Chen G Zhao X 2021 Studies on friction and wear characteristics of wire rope used in multi-layer winding hoist during inter-circle transition under dry friction. *Proc. Inst. Mech. Eng.* **236**(1) 90–104
[24] Krešák K Peterka P Ambriško L and Mantič M 2021 Friction lining coefficient of the drive friction pulley, *Eksploatacja I Niezawodność* **23**(2) 338–45
[25] Jordan D W Smith P 1999 Nonlinear ordinary differential equations: An Introduction to Dynamical Systems. Oxford University Press USA

[26] Bhushan B 2001 Modern Tribology Handbook: Materials, coatings, and industrial applications
[27] Timoshenko 2007 Engg Mechanics Revsd 4E Sie Tata McGraw-Hill Education
[28] Blau P J 1996 Needs and challenges in precision wear measurement Oak Ridge National Lab. (ORNL), Oak Ridge, TN USA Jan